Computers and Structures 120 (2013) 24–32

Contents lists available at SciVerse ScienceDirect

Computers and Structures

journal homepage: www.elsevier.com/locate/compstruc

Stochastic structural dynamic analysis using Bayesian emulators

F.A. DiazDelaO [a,*], S. Adhikari [a], E.I. Saavedra Flores [a,b], M.I. Friswell [a]

[a] Civil and Computational Engineering Centre, College of Engineering, Swansea University, Singleton Park, Swansea SA2 8PP, United Kingdom
[b] Departamento de Ingeniería en Obras Civiles, Universidad de Santiago de Chile, Av. Ecuador 3659, Santiago, Chile

ARTICLE INFO

Article history:
Received 7 August 2012
Accepted 21 January 2013

Keywords:
Metamodel
Gaussian process emulator
Structural dynamics
Stochastic finite element method
Homogenisation
Composite materials

ABSTRACT

The probabilistic characterisation of a frequency response function can be very valuable for structural design and control. Unfortunately, obtaining a sufficiently large sample for wide ranges of vibration can easily become unaffordable. A variety of modelling assumptions can dramatically add to the computational cost: nonproportional damping, multiscale material properties, and high-resolution finite element analysis are some examples. This paper explores Bayesian emulators as surrogates for expensive finite element models in structural dynamics. We demonstrate the effectiveness of the method by performing uncertainty analysis of the frequency response of a nonproportionally damped plate made of a carbon fibre/epoxy composite material.

1. Introduction

The consideration of uncertainties in numerical models to obtain probabilistic descriptions of the vibration response is becoming more desirable for industrial-scale finite element models. Very large finite element models [1,2] are used for complex engineering dynamical systems such as helicopters, automobiles and aircraft. For mid and high-frequency applications, the calculation of response is necessary for a wide range of frequency. Larger size models, the consideration of uncertainty and a wide frequency range of interest make stochastic structural dynamics particularly challenging for computational methods. Stochastic finite element-based methods [3–9] have been proposed for uncertainty propagation in static or low-frequency vibration problems. For dynamic problems, perturbation-based approaches utilising random eigenvalue problems [10,11] have been used for the forced vibration response of linear dynamical systems. These methods are, however, normally restricted to low levels of random variation in the parameters. This problem can be avoided if a simulation-based approach is adopted. The disadvantage is that a direct Monte Carlo approach can be computationally expensive. In this paper we develop an efficient simulation approach based on Gaussian process emulators for the frequency response function (FRF) of stochastic dynamical systems.

A computer code or implementation of a mathematical model, also known as a simulator [12], can be understood as a function $\eta : \Omega \to \mathbb{R}^d$ whose domain is an input space Ω. A simulator is deterministic whenever the same input $\omega \in \Omega$ results in the same output $\mathbf{y} = \eta(\omega)$. Deterministic simulators are widely used in science and engineering to represent and study intricate phenomena. However, complex models can be too computationally intensive, in which case it is common to employ less expensive approximations. In the literature, these approximations are known as surrogate models, metamodels, response surfaces, or auxiliary models, among others [13–20]. One such surrogate modelling strategy, known as Gaussian process emulation, is based on the analysis and design of computer experiments [21,22] and on the concepts of Bayesian statistics. Using this approach, it is possible to obtain a statistical approximation to the output of a simulator after evaluating a small number n of design points $\{\omega_i\}_{i=1}^n$ in the input domain Ω, hence reducing the required computer processing time. Broadly speaking, the emulation works by generating a small set of training runs $\{\omega_i, \eta(\omega_i)\}_{i=1}^n$ that are treated as data used to update some prior beliefs about the simulator's output. These beliefs are represented by a Gaussian stochastic process prior distribution. After conditioning on the training runs and updating the prior distribution, the mean of the resulting posterior distribution approximates the output of the simulator at any untried input $\omega \in \Omega$, whereas it reproduces the known output at each design point. Gaussian process emulators have been implemented in various scientific fields in order to alleviate the computational burden of expensive simulators with encouraging results. These fields include climate prediction [23,24], environmental science [25], medicine [26–28], deterministic structural dynamics [29], stochastic structural dynamics [30], reservoir forecasting [31], hydrogeology [32], quality control [33], heat transfer [34], multi-scale analysis [35], stochastic finite elements [36], and domain decomposition [37] among many others.

* Corresponding author. Tel.: +44 (0)1792 513177; fax: +44 (0)1792 295157.
E-mail address: f.a.diazdelao@swansea.ac.uk (F.A. DiazDelaO).

0045-7949/$ - see front matter © 2013 Elsevier Ltd. All rights reserved.
http://dx.doi.org/10.1016/j.compstruc.2013.01.013

In this paper we study the application of Gaussian process emulation to the frequency response of complex engineering dynamical systems in the presence of uncertainty. The choice of the finite element method is based on its wide range of applicability in different kinds of problems such as static problems, modal analysis and stability analysis [38]. This paper follows previous work on the emulation of a deterministic frequency response [29], that is, the FRF depends only on the frequency level and not on any stochastic parameter. An earlier study of emulators in the context of stochastic structural dynamics can be found in [30], where the FRF of an aircraft model was emulated. In their study, the authors focus on an undamped FRF. Additionally, they mention that their choice of the uncertain parameters (and their distributions) is somewhat arbitrary. In this paper, we choose nonproportional damping as one of the sources of numerical cost. In addition to this, the probability distribution of the random parameter results from an homogenisation approach, which takes into account a realistic physical description of the material under study. This work can also be considered a refinement of the approach in [37]. In that paper, the design points upon which the emulator is built are not assumed to follow any particular probabilistic structure. In this paper, the inputs follow a probability distribution determined by the physical properties of the structure under study. It is thanks to that probabilistic nature that it is possible to sample from the input space in order to estimate statistical summaries of the output, despite the computational cost.

The paper is organised as follows: In Section 2, the motivation of this study is established. The FRF of a simple spring-mass system is used as an introductory example. In Section 3, the general theory behind Gaussian process emulators is briefly reviewed. Section 4 discusses how to perform the analysis of the uncertainty propagated by a simulator using Gaussian process emulators. In Section 5, an expensive finite element simulator of the frequency response of a plate is studied. Finally, Section 6 offers some conclusions.

2. Motivation for the present study

In the context of stochastic structural dynamics, let the relevant simulator be represented by $\eta : \Omega \times \Theta \to \mathbb{R}$, where $\Omega \subseteq [0,\infty)$ contains frequency levels ω and Θ is the set of realisations of a random parameter θ. The output of the simulator is the FRF of the system. Some authors [12] note that, even if θ is a random parameter, the distinction between stochastic and deterministic simulators is artificial: when implemented numerically, a set of realisations of θ is a sequence of pseudo-random numbers. Thus, for a fixed seed that initialises the pseudo-random number generator, such a sequence is deterministic. Suppose that a statistic of the output $\eta(\omega,\theta)$, such as the mean, the variance, or a specific percentile, is to be obtained. This task may easily become burdensome, since even obtaining a few instances of the desired statistic would require $\eta(\omega,\theta)$ to be evaluated at each frequency level repeatedly for a potentially large number, S, of realisations of θ.

Consider the nonproportionally damped [39] spring-mass system shown in Fig. 1. Suppose for the time being that the simulator of the corresponding FRF is computer intensive and that there is no parametric uncertainty. To obtain the FRF, we begin with the equation of motion of a damped M-degree-of-freedom linear structural system [40,41], given by

$$\mathbf{M}\ddot{\mathbf{u}}(t) + \mathbf{C}\dot{\mathbf{u}}(t) + \mathbf{K}\mathbf{u}(t) = \mathbf{f}(t) \tag{1}$$

where $\mathbf{f}(t) \in \mathbb{R}^M$ is the forcing vector, $\mathbf{u}(t) \in \mathbb{R}^M$ is the response vector and $\mathbf{M}$, $\mathbf{C}$, $\mathbf{K} \in \mathbb{R}^{M\times M}$ are respectively the mass, damping and stiffness matrices.

Eq. (1) can be expressed in terms of the excitation frequency level ω as

$$\mathbf{D}(\omega)\bar{\mathbf{u}}(\omega) = \bar{\mathbf{f}}(\omega) \tag{2}$$

where $\bar{\mathbf{u}}(\omega)$ and $\bar{\mathbf{f}}(\omega)$ are the Fourier transforms of $\mathbf{u}$ and $\mathbf{f}$ respectively. The complex symmetric matrix $\mathbf{D}(\omega)$, known as the dynamic stiffness matrix, is given by

$$\mathbf{D}(\omega) = -\omega^2\mathbf{M} + \mathrm{i}\omega\mathbf{C} + \mathbf{K} \tag{3}$$

where i is the unit imaginary number. If $\mathbf{D}(\omega)$ is non-singular, then the response vector is $\bar{\mathbf{u}}(\omega) = \mathbf{D}(\omega)^{-1}\bar{\mathbf{f}}(\omega)$. $\mathbf{D} \in \mathbb{C}^{M\times M}$, but often only the moduli of the response vector components are relevant in practice. Hence the simulator of the FRF is

$$\eta(\omega) = |[-\omega^2\mathbf{M} + \mathrm{i}\omega\mathbf{C} + \mathbf{K}]^{-1}\bar{\mathbf{f}}(\omega)| \tag{4}$$

The domain Ω of Eq. (4) is the set of possible values of the frequency level ω. The cardinality of Ω (denoted by $|\Omega|$) depends on the size and resolution of the frequency domain, e.g. 1 to 100 Hz with increments of 1 Hz. Let the mass of each block be 0.8 kg, the stiffness of each spring be 1 N m^{-1}, and the viscous damping constant associated with each block be 0.2 N s m^{-1}. It can be shown that the mass, stiffness and damping matrices of this simple system are

$$\mathbf{M} = \begin{pmatrix} m & 0 & 0 \\ 0 & m & 0 \\ 0 & 0 & m \end{pmatrix} \quad \mathbf{K} = \begin{pmatrix} 2k & -k & 0 \\ -k & 2k & -k \\ 0 & -k & 2k \end{pmatrix} \quad \mathbf{C} = \begin{pmatrix} c & 0 & 0 \\ 0 & 0 & 0 \\ 0 & 0 & c \end{pmatrix} \tag{5}$$

where m = 0.8 kg, k = 1 N m^{-1}, and c = 0.2 N s m^{-1}. Assume the forcing vector is $\mathbf{f} = [0,1,0]^\top$ N.

Suppose that we introduce uncertainty to the governing equation of the dynamical system shown in Fig. 1. This would be justified because uncertainty is practically unavoidable in the realistic description of most physical systems [42,43]. Randomness can be introduced by uncertain material properties, uncertain boundary conditions or unknown manufacturing tolerances. Suppose that any of the matrices in Eq. (1) is a random matrix, that is, it includes a random parameter $\theta \in \Theta$. Without loss of generality, if the stiffness matrix $\mathbf{K}$ is random, then Eq. (4) becomes

$$\eta(\omega,\theta) = |[-\omega^2\mathbf{M} + \mathrm{i}\omega\mathbf{C} + \mathbf{K}(\theta)]^{-1}\bar{\mathbf{f}}(\omega)| \tag{6}$$

where

$$\mathbf{K}(\theta) = \begin{pmatrix} 2k(\theta) & -k(\theta) & 0 \\ -k(\theta) & 2k(\theta) & -k(\theta) \\ 0 & -k(\theta) & 2k(\theta) \end{pmatrix} \tag{7}$$

The domain of Eq. (6) is $\Omega \times \Theta$, where Ω is the set of admissible frequency levels and Θ is the set of realisations of the random parameter θ. As noted before, a fixed seed implies that the simulator in Eq. (6) is deterministic, as it produces the same (scalar) output given the same stream of pseudo-random numbers. For notational convenience, the seed does not appear explicitly as a parameter of the simulator. Fig. 2(a) shows S = 150 realisations of the spring-mass FRF for the third degree of freedom, where $\omega \in \Omega = \{0, 0.01, \ldots, 2.99, 3\}$ and θ is assumed to be uniformly distributed in $\Theta = [0.9, 1.1]$. Additional to the 150 realisations of $\eta(\omega,\theta)$, the mean FRF (the dotted line) for all $\omega \in \Omega$ is shown. The direct calculation of the mean model output would involve 150×301 evaluations of $\eta(\omega,\theta)$.

The metamodelling scheme explored in this paper is based on observing that the input domain $\Omega \times \Theta$ offers the possibility of sampling the design points from Θ, whilst fixing those in Ω. That is, if the output of the simulator $\eta(\omega,\theta)$ is treated as a function of θ only, then it is possible to build an emulator at every point in Ω

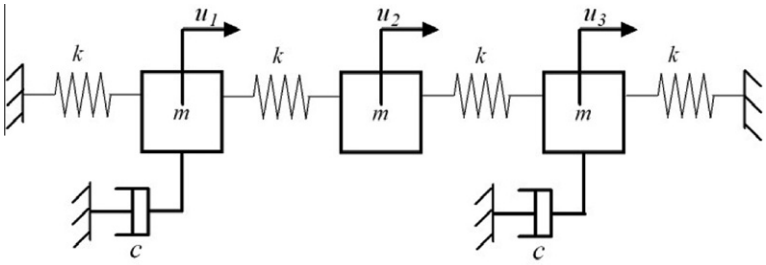

Fig. 1. Three-degree-of-freedom nonproportionally damped spring-mass system; $m = 0.8$ kg, $k = 1$ N m^{-1}, $c = 0.2$ N s m^{-1}.

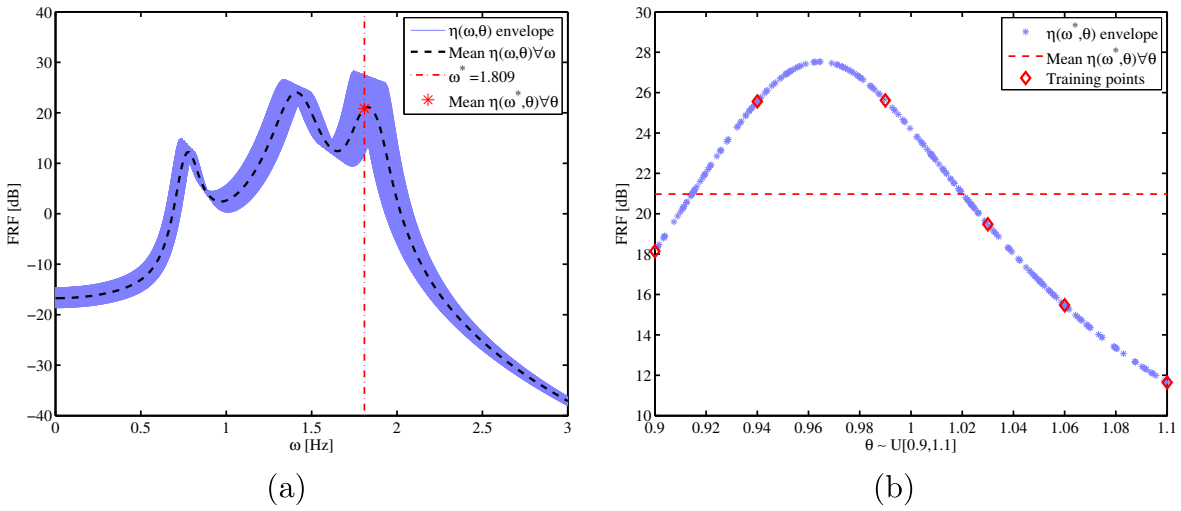

Fig. 2. 150 Realisations of the frequency response function of the third degree of freedom of a spring-mass system, with $\omega \in \Omega = \{0{,}0.01,\ldots,2.99{,}3\}$, $\theta \sim U[0.9, 1.1]$. (a) Realisations of $\eta(\omega,\theta)$ and mean output; (b) realisations of $\eta(\omega^*,\theta)$ and mean output.

and approximate a statistic of interest using design points taken from Θ. If the number of selected design points per emulator is less than S, then the total number of evaluations of $\eta(\omega,\theta)$ is reduced. Fig. 2(a) illustrates this idea. For ω^* fixed, the mean of 150 realisations of $\eta(\omega^*,\theta)$ is a point on the mean FRF curve. On the other hand, Fig. 2(b) shows the same 150 realisations and their mean (the dotted straight line), this time with θ as the abscissas. For illustration purposes, consider choosing 6 design points from Θ (the diamonds). Using these training runs, a Gaussian process emulator could approximate the realisations of $\eta(\omega^*,\theta)$ and the mean of the resulting values would in turn be used to approximate the mean output at ω^*. If the same procedure is followed for every $\omega \in \Omega$, then $\eta(\omega,\theta)$ would be evaluated 6×301 times. This represents only 4% of the original computational effort. Additionally, if the time taken to emulate the statistic for every point in Ω is reasonably short, there might be an improvement in the overall computer processing time required. In practice, the choice of the number of design points greatly depends on the smoothness of the function to be emulated and the computational resources available.

3. Brief overview of Gaussian process emulators

3.1. Basic definitions

Let $\eta(\omega,\theta)$ be an expensive deterministic simulator, such that the cost of running it is affordable only at a limited number of input points. The uncertainty about the output of $\eta(\omega,\theta)$ can be described through a probability distribution [44]. It is common to assume the following stochastic representation

$$\eta(\omega,\theta) = \mathbf{h}(\omega,\theta)^\top \boldsymbol{\beta} + Z(\omega,\theta) \tag{8}$$

where $\mathbf{h}(\omega,\theta)$ is a vector of known functions and $\boldsymbol{\beta}$ is a vector of unknown coefficients. Some authors [27,45] note that $\mathbf{h}(\omega,\theta)$ should be chosen to reflect the available information about the functional form of $\eta(\omega,\theta)$. Other authors [13] consider that a constant mean (that is $\mathbf{h} = 1$) is flexible enough to capture complex functional relationships. In this paper we adopt this view. The function $Z(\omega,\theta)$ is a stochastic process with mean zero and correlation function $C[(\omega,\theta),(\omega,\theta')]$. Let $\mathbf{y} = [\eta(\omega_1,\theta_1),\ldots,\eta(\omega_n,\theta_n)]^\top$ be a vector of observations corresponding to the design points $\{(\omega_i,\theta_i)\}_{i=1}^n$. These observations are used to update the prior distribution of the simulator. An analytically convenient choice for the prior is the following Gaussian process distribution [26]

$$\eta(\omega,\theta)|\boldsymbol{\beta},\sigma^2 \sim \mathcal{N}(\mathbf{h}(\omega,\theta)^\top\boldsymbol{\beta}, \sigma^2 C[(\omega,\theta),(\omega,\theta)]) \tag{9}$$

where $\mathbf{h}(\omega,\theta)$ and $\boldsymbol{\beta}$ are defined as above. The correlation function $C[(\omega,\theta),(\omega,\theta')]$ is such that

$$C[(\omega,\theta),(\omega,\theta')] = \exp\left\{-[(\omega,\theta)-(\omega,\theta')]^\top \mathbf{B}[(\omega,\theta)-(\omega,\theta')]\right\} \tag{10}$$

where $\mathbf{B}$ is a diagonal positive definite matrix. The diagonal of $\mathbf{B}$ is a vector $\mathbf{b} \in \mathbb{R}^n$ of smoothness parameters. These parameters quantify the rate at which the output varies as the input varies. In order to estimate them, a density function $f(\mathbf{B}|\mathbf{y})$ can be derived and a maximum likelihood estimator obtained [46]. The choice of a Gaussian process is made for much the same reasons that Gaussian distributions are so frequently used in statistics: they are convenient, flexible and quite often realistic [47]. This does not imply that uncertainty (v.g. geometric, material) in the physical system being emulated is necessarily assumed to be Gaussian. However, the flex-

ibility of the Gaussian process allows the emulation of complex input/output relationships.

After conditioning on the training runs and updating the prior distribution (9), the mean of the resulting posterior distribution approximates the output of $\eta(\omega,\theta)$ at any untried input (ω,θ), and reproduces the known output at each design point $\{(\omega_i,\theta_i)\}_{i=1}^n$. The variance of the posterior distribution quantifies the uncertainty that arises from having only a limited number of evaluations of $\eta(\omega,\theta)$ [24]. Very conveniently, the posterior is also a Gaussian process distribution, obtained as follows: Let $\mathbf{H}=[\mathbf{h}(\omega_1,\theta_1),\ldots,\mathbf{h}(\omega_n,\theta_n)]^\top$, and $\mathbf{A}\in\mathbb{R}^{n\times n}$ such that $\mathbf{A}_{ij}=C[(\omega_i,\theta_i),(\omega_j,\theta_j)]\ \forall i,j\in\{1,\ldots,n\}$. Then

$$\mathbf{y}|\boldsymbol{\beta},\sigma^2\sim\mathcal{N}(\mathbf{H}\boldsymbol{\beta},\sigma^2\mathbf{A}) \tag{11}$$

To incorporate the information $\mathbf{y}$ and obtain the distribution of $\eta(\omega,\theta)|\mathbf{y}$, we use the following theorem, a demonstration of which can be found in [48].

Theorem 1. *Let* $\mathbf{z}\in\mathbb{R}^N$ *be a random vector such that* $\mathbf{z}\sim\mathcal{N}(\boldsymbol{\mu},\Sigma)$. Partition $\mathbf{z}$ as $(\mathbf{z}_1,\mathbf{z}_2)^\top$, *where* $\mathbf{z}_1\in\mathbb{R}^{N-n}$ and $\mathbf{z}_2\in\mathbb{R}^n$. Consequently, partition $\mu=(\mu_1,\mu_2)^\top$ and $\Sigma=\begin{pmatrix}\Sigma_{11}&\Sigma_{12}\\ \Sigma_{21}&\Sigma_{22}\end{pmatrix}$, so that $\mathbf{E}[\mathbf{z}_j]=\mu_j$ *and* $\mathrm{Cov}(\mathbf{z}_j,\mathbf{z}_k)=\Sigma_{jk}$. *Then,* $\mathbf{z}_1|\mathbf{z}_2\sim\mathcal{N}(\widetilde{\boldsymbol{\mu}},\widetilde{\Sigma})$, *where* $\widetilde{\boldsymbol{\mu}}=\boldsymbol{\mu}_1+\Sigma_{12}\Sigma_{22}^{-1}(\mathbf{z}_2-\boldsymbol{\mu}_2)$ *and* $\widetilde{\Sigma}=\Sigma_{11}-\Sigma_{12}\Sigma_{22}^{-1}\Sigma_{21}$.

It follows that

$$\eta(\omega,\theta)|\mathbf{y},\boldsymbol{\beta},\sigma^2\sim\mathcal{N}(m^*(\omega,\theta),\sigma^2C^*[(\omega,\theta),(\omega,\theta)]) \tag{12}$$

where

$$m^*(\omega,\theta)=\mathbf{h}(\omega,\theta)^\top\boldsymbol{\beta}+\mathbf{t}(\omega,\theta)^\top\mathbf{A}^{-1}(\mathbf{y}-\mathbf{H}\boldsymbol{\beta}) \tag{13}$$

$$C^*[(\omega,\theta),(\omega,\theta')]=C[(\omega,\theta),(\omega,\theta')]-\mathbf{t}(\omega,\theta)^\top\mathbf{A}^{-1}\mathbf{t}(\omega,\theta') \tag{14}$$

$$\mathbf{t}(\omega,\theta)=[C[(\omega,\theta),(\omega_1,\theta_1)],\ldots,C[(\omega,\theta),(\omega_n,\theta_n)]]^\top \tag{15}$$

Removing the conditioning on $\boldsymbol{\beta}$ using standard integration techniques [26], we obtain the posterior distribution

$$\eta(\omega,\theta)|\mathbf{y},\sigma^2\sim\mathcal{N}(m^{**}(\omega,\theta),\sigma^2C^{**}[(\omega,\theta),(\omega,\theta)]) \tag{16}$$

where

$$m^{**}(\omega,\theta)=\mathbf{h}(\omega,\theta)^\top\widehat{\boldsymbol{\beta}}+\mathbf{t}(\omega,\theta)^\top\mathbf{A}^{-1}(\mathbf{y}-\mathbf{H}\widehat{\boldsymbol{\beta}}) \tag{17}$$

$$\begin{aligned}C^{**}[(\omega,\theta),(\omega,\theta')]=C^*[(\omega,\theta),(\omega,\theta')]+(\mathbf{h}(\omega,\theta)^\top\\ -\mathbf{t}(\omega,\theta)^\top\mathbf{A}^{-1}\mathbf{H})(\mathbf{H}^\top\mathbf{A}^{-1}\mathbf{H})^{-1}(\mathbf{h}(\omega,\theta')^\top\\ -\mathbf{t}(\omega,\theta')^\top\mathbf{A}^{-1}\mathbf{H})^\top\end{aligned} \tag{18}$$

$$\widehat{\boldsymbol{\beta}}=(\mathbf{H}^\top\mathbf{A}^{-1}\mathbf{H})^{-1}\mathbf{H}^\top\mathbf{A}^{-1}\mathbf{y} \tag{19}$$

To estimate σ in Eq. (16), let q be the rank of $\mathbf{H}$. Then

$$\widehat{\sigma}^2=\frac{\mathbf{y}^\top(\mathbf{A}^{-1}-\mathbf{A}^{-1}\mathbf{H}(\mathbf{H}^\top\mathbf{A}^{-1}\mathbf{H})\mathbf{H}^\top\mathbf{A}^{-1})\mathbf{y}}{n-q-2} \tag{20}$$

Finally, it can be shown that

$$\frac{\eta(\omega,\theta)-m^{**}(\omega,\theta)}{\widehat{\sigma}\sqrt{\frac{(n-q-2)C^{**}(\omega,\theta)}{n-q}}}\sim t_{n-q} \tag{21}$$

which is a Student's t-distribution with $n-q$ degrees of freedom (not to be confused with the degrees of freedom in a finite element method context).

From the above discussion, it can be seen that Gaussian process emulation consists in updating the prior distribution (9), which contains subjective information, by adding the objective information $\mathbf{y}$ in order to obtain the posterior distribution (16). This enables the calculation of the predictive mean $m^{**}(\omega,\theta)$ given the data $\mathbf{y}$. This mean is a fast approximation of $\eta(\omega,\theta)$ for any (ω,θ) in the input domain.

As mentioned before, the simulator can be treated as function of θ only. For a fixed ω^*, an emulator can be built as outlined in Algorithm 1.

Algorithm 1. Gaussian process emulation

Input: Design points $\{(\omega^*,\theta_i)\}_{i=1}^n$ for a fixed ω^*
Output: Predictive mean $m^{**}(\omega^*,\theta)\equiv\mathbf{E}[\eta(\omega^*,\theta)|\mathbf{y}]$ and variance $\sigma^2C^{**}[(\omega^*,\theta),(\omega^*,\theta)]\equiv\mathbf{Var}[\eta(\omega^*,\theta)|\mathbf{y}]$
begin
1. Select n design points $\{(\omega^*,\theta_i)\}_{i=1}^n$
2. Obtain the vector of observations $\mathbf{y}=[\eta(\omega^*,\theta_1),\ldots,\eta(\omega^*,\theta_n)]^\top$
3. Update the prior distribution (9) using $\mathbf{y}$ and obtain the posterior distribution (16)
4. Compute $m^{**}(\omega^*,\theta)$ and $\sigma^2C^{**}[(\omega^*,\theta),(\omega^*,\theta)]$ for any untried (ω^*,θ)

end

4. Uncertainty propagation

4.1. FRF statistics

Consider a dynamical system whose FRF is simulated by Eq. (6). Suppose that we wish to obtain a statistic of the FRF, such as the mean or the variance. Let $|\Omega|=N$ and $\ell\in\{1,\ldots,N\}$. Also, let $\{\theta_s^\ell\}_{s=1}^S=\{\theta_1^\ell,\ldots,\theta_S^\ell\}$ be a set of realisations of a random parameter θ associated to a fixed frequency level ω_ℓ in $\Omega=\{\omega_\ell\}_{\ell=1}^N$. Then, at every ω_ℓ the mean FRF is estimated by

$$\widehat{\eta}_1(\omega_\ell,\theta_1^\ell,\ldots,\theta_S^\ell)=\frac{1}{S}\sum_{s=1}^S\eta(\omega_\ell,\theta_s^\ell) \tag{22}$$

whereas the variance of the FRF is estimated by

$$\widehat{\eta}_2(\omega_\ell,\theta_1^\ell,\ldots,\theta_S^\ell)=\frac{1}{S-1}\left[\sum_{s=1}^S\eta^2(\omega_\ell,\theta_s^\ell)-\left[\frac{1}{S}\sum_{s=1}^S\eta(\omega_\ell,\theta_s^\ell)\right]^2\right] \tag{23}$$

The most straightforward approach to estimate $\widehat{\eta}_1$ and $\widehat{\eta}_2$ is Monte Carlo simulation (MCS): For $\ell=1,\ldots,N$, simulate $\{\eta(\omega_\ell,\theta_s^\ell)\}_{s=1}^S$ and compute Eq. (22) or Eq. (23). The number of evaluations of $\eta(\omega,\theta)$ would be $S\cdot N$. Nevertheless, if $\eta(\omega,\theta)$ is computationally expensive, MCS can quickly become impracticable. Observe however that the input domain $\Omega\times\Theta$ allows the sampling of design points from Θ for every frequency level in Ω. That way, the number of evaluations can be reduced: For $\ell=1,\ldots,N$, generate L_ℓ design points $\left\{\theta_j^\ell\right\}_{j=1}^{L_\ell}$. Then, compute the training runs $\left\{\theta_j^\ell,\eta(\omega_\ell,\theta_j^\ell)\right\}_{j=1}^{L_\ell}$ and emulate p runs $\{\eta(\omega_\ell,\theta_k^\ell)\}_{k=1}^p$ at each of the untried inputs $\left\{\theta_1^\ell,\ldots,\theta_p^\ell\right\}$. The number of evaluations of $\eta(\omega,\theta)$ would be $L=L_1+\cdots+L_N$. If $L<S$, the computational burden of evaluating $\eta(\omega,\theta)$ would is reduced compared to Monte Carlo simulation, since $L<S\Rightarrow L<S\cdot N$.

In the procedure described above, for every frequency level ω_ℓ, the design points $\left\{\theta_j^\ell\right\}_{j=1}^{L_\ell}$ are realisations of a random parameter and therefore are drawn from a probability distribution $\mathcal{F}_\Theta(\theta)$. Such distribution can be specified or elicited through expert opinion. The uncertainty in this input distribution is propagated through the simulator $\eta(\omega,\theta)$. Our aim is to characterise the resulting output distribution $\mathbf{Y}=\eta(\omega,\theta)$. If $\eta(\omega,\theta)$ were not an expensive simulator, the most straightforward uncertainty analysis would be

to draw a large sample or realisations of θ from the input distribution $\mathcal{F}_\Theta(\theta)$ and then run the simulator in each of them. This would result in a sample of outputs from which any statistic $\mathfrak{S}(\mathbf{Y})$ could be estimated as in Eq. (22) or Eq. (23). In principle, the predictive mean $m^{**}(\omega,\theta)$ of a Gaussian process emulator could be used as a direct replacement of $\eta(\omega,\theta)$ in order to carry out the simple uncertainty analysis just described. However, $m^{**}(\omega,\theta)$ is only an approximation to $\eta(\omega,\theta)$, and therefore this approach does not incorporate the corresponding uncertainty. The solution to this problem was proposed by Oakley and O'Hagan [49] with a modified Monte Carlo procedure summarised in Algorithm 2. In our case, the algorithm is applied for every $\omega_\ell \in \Omega$.

Algorithm 2. GPE uncertainty analysis

Input: Sample $\{\theta_i\}_{i=1}^{L_\ell}$ from the input distribution $\mathcal{F}_\Theta(\theta)$
Output: Summary $\mathfrak{S}(\mathbf{Y})$ of the output distribution $\mathbf{Y}$
begin
1. Draw a sample $\{\theta_i\}_{i=1}^{L_\ell}$ from the distribution $\mathcal{F}_\Theta(\theta)$
2. Draw a random function $\eta_{(j)}$ from the emulator posterior distribution (16)
3. Evaluate $\eta_{(j)}(\theta_1),\ldots,\eta_{(j)}(\theta_{L_\ell})$
4. Obtain $\mathfrak{S}_j(\mathbf{Y})$, the Monte Carlo estimate of $\mathfrak{S}(\mathbf{Y})$
5. Repeat steps 2–4 and obtain the sample $\{\mathfrak{S}_1(\mathbf{Y}),\ldots,\mathfrak{S}_{N_\eta}(\mathbf{Y})\}$
6. Use the sample obtained in step 5 to estimate any summary of the distribution of $\mathfrak{S}(\mathbf{Y})$

end

4.2. Nonparametric regression

The strategy described above can be used to generate statistical summaries of the FRF for a finite set of frequencies $\omega_1,\ldots,\omega_N$ in Ω. Suppose that, additionally, we wanted to estimate statistics of the FRF for any frequency level in the interval $[\omega_1,\omega_N]$. Clearly, a pointwise approach like the one described so far would be unfeasible. We propose to solve this by running a Gaussian process regression based on the data set $\{(\omega_\ell,\mathcal{S}(\omega_\ell))|\ell=1,\ldots,N\}$, where each $\mathcal{S}(\omega_\ell)$ is the statistic computed using uncertainty analysis previously discussed. This is a type of non-parametric regression, in the sense that we are not constraining the unknown function to belong to a prescribed functional family (linear, for example). It can be shown [50] that, analogously to Eq. (10), the covariance function will be of the form

$$Cov(W(\omega,\theta),W(\omega',\theta))) = \sigma_w^2 C(\omega,\omega') + \boldsymbol{\Sigma} \tag{24}$$

where $W(\omega,\theta)$ is a Gaussian process and $\boldsymbol{\Sigma}$ is a diagonal matrix with $[\boldsymbol{\Sigma}]_{ii} = \sigma_i^2$. We can readily estimate the variances $\{\sigma_1^2,\ldots,\sigma_N^2\}$ with the uncertainty analysis provided by Algorithm 2.

Summarizing, for every ω in Ω (which is a finite set), we draw design points from Θ, evaluate the simulator to obtain training runs, and estimate a summary of the FRF. We then use those estimates as new training runs and provide an estimate of the summary for any ω between ω_1 and ω_N.

5. Numerical investigation: nonproportionally damped plate made of a composite material

In the introductory example in Section 2, the uncertainty in the stiffness matrix $\mathbf{K}(\theta)$ in Eq. (6) was assumed to depend in a uniformly distributed parameter θ. This choice, although illustrative, was made arbitrarily. In this section, we present a model in which the uncertainty in the stiffness is determined by the microstructure of a composite material. We assume this material to be defined by carbon fibres embedded in an epoxy matrix, such that there is uncertainty in the diameter of each fibre. This uncertainty is explicitly modelled and then propagated through a finite element code. This propagation results in an uncertain FRF, the mean and variance of which we aim to estimate. We employ a homogenisation-based multiscale model to compute the mechanical response of the material and we assume the presence of nonproportional damping.

5.1. Finite element modelling

In order to implement the metamodelling strategy outlined in Section 4, consider a square plate. The plate is excited by an unit harmonic force and the frequency response is measured at one of the nodes. The geometric and physical properties are: length 1 m, width 1 m and thickness 1 mm. A finite element model of the plate is shown in Fig. 3(b). We assume that the plate has a damping patch attached. The resulting damping is nonproportional. The calculation of the FRF for this kind of nonproportionally damped systems can be very expensive [51,52]. In general, it is not possible to represent the response in terms of undamped modes. In such cases the response needs to be expressed in terms of the complex modes of the system [53]. Even for a relatively small case, solving the linear system (2) for each frequency level can be very resource-consuming.

5.2. Material modelling

The material is assumed to be a carbon fibre/epoxy composite whose overall mechanical response is obtained by the computational homogenisation of the representative volume element (RVE) shown in Fig. 3(a). To capture the actual mechanical response of the composite material, we adopt a framework based on the periodic boundary displacement fluctuations model [54], widely adopted in the modelling of periodic media. This type of model offers the possibility to describe more accurately the stress response under complex strain paths, although it suffers from the drawback of excessive computing costs. These costs are usually acceptable when finite element analyses of single RVEs are carried out in the context of deterministic problems (refer, for instance, to Refs. [55–57]). However, when parametric uncertainty is considered in the context of multiscale problems, the computational cost of solving the computer model may rise by several orders of magnitude when compared to deterministic single-scale analyses. For more details about homogenisation-based multiscale constitutive theory, refer to Appendix A.

We consider a periodic linear elastic medium with circular reinforcing fibres distributed uniformly. Following [58], for the carbon fibres we assume an isotropic material with Young's modulus $E = 235$ GPa and Poisson's ratio $\nu = 0.2$. The longitudinal direction of the fibres coincides with the X axis shown in Fig. 3. The transverse directions of the material are defined by the Y and Z axes. The epoxy material is assumed to be isotropic with Young's modulus $E = 4.6$ GPa and Poisson's ratio $\nu = 0.36$ [58]. A typical finite element mesh consists of 23,471 nodes and 93,776 four-noded linear tetrahedral elements. Since the density of the carbon fibres and the epoxy matrix is similar, we adopt the same value for both materials, namely 1.5 kg/m^3.

5.3. Uncertainty modelling

In order to introduce uncertainty in the material definition, we propose a modelling strategy which perturbs the diameter of each fibre shown in Fig. 3(a). Since we are interested in calculating the overall mechanical properties of the composite, all the diameters are perturbed simultaneously about a baseline value, resulting in a first set of homogenised elastic properties. In this study, the baseline value for the corresponding diameters of each fibre is ta-

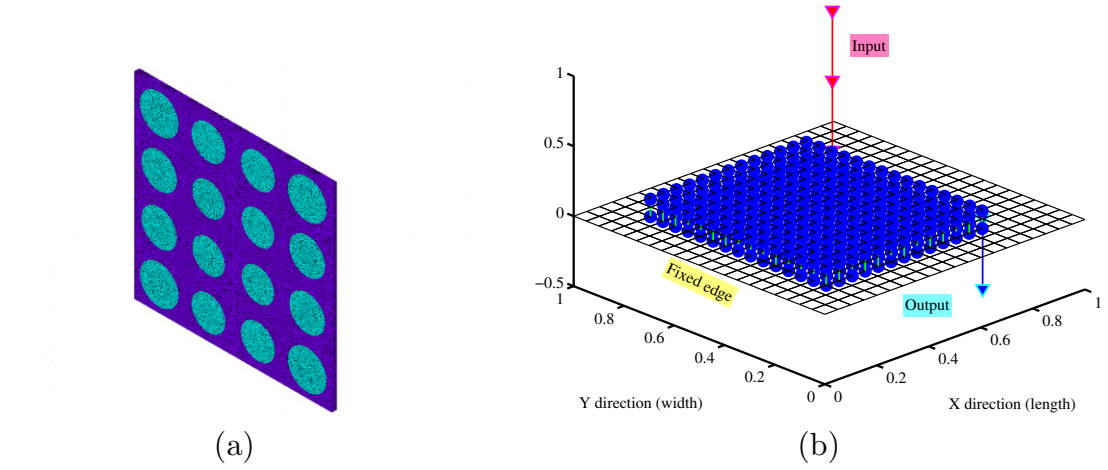

Fig. 3. Finite element model of a composite plate with a damping patch. The material and geometric properties are: length 1 m, width 1 m, thickness 1 mm. A microscopic finite element mesh was adopted for the computation of the homogenised mechanical properties of the composite material. (a) Microscopic FE model; (b) macroscopic FE model.

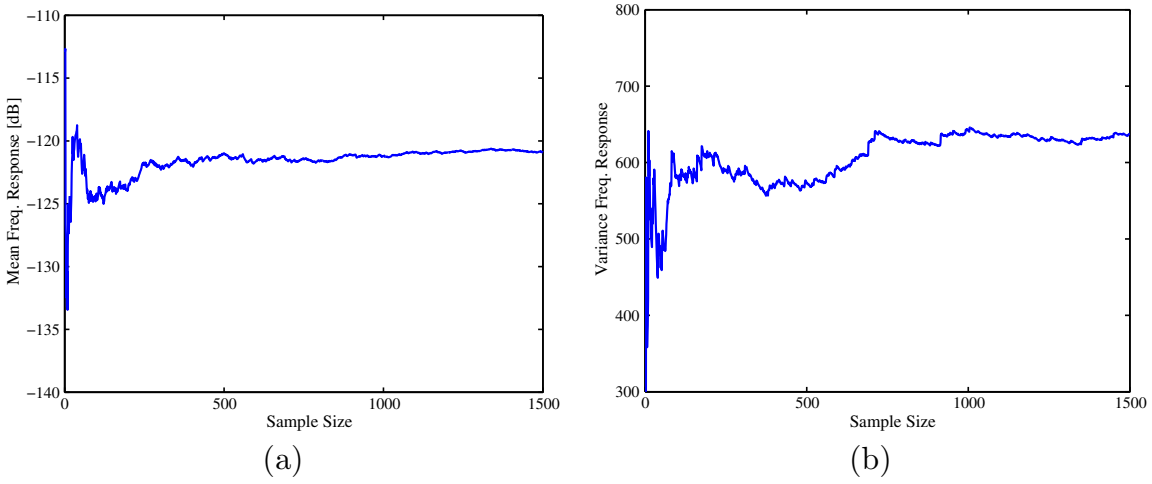

Fig. 4. Mean (a) and variance (b) of the frequency response function (FRF) at $\omega = 71$ Hz for different sample sizes. Both statistics seem to stabilise for sample sizes greater than or equal to 1000.

ken as 17.84% of the unit side of the RVE. This results in a baseline volume fraction of 0.40 (refer to [59]). The assumed input distribution for each diameter is chosen to be Gaussian with a mean equal to the baseline value and with a variance such that 8.89% of the baseline value equals 1 standard deviation [59]. Consequently, for each fibre, the diameter d_i is distributed as $d_i \sim \mathcal{N}(0.1784, [0.0889 \times 0.1784]^2)$ and thus each radius r_i is distributed as $r_i \sim \mathcal{N}(0.0892, 0.0079^2)$. The procedure is repeated again, for a second set of homogenised mechanical properties, and so on. We then take the volume fraction as the random parameter θ. The uncertainty induced by this random volume fraction is propagated through the finite element model such that, for every realisation of θ, we obtain an FRF for a predetermined range of vibration. While the probability distribution of the radii were taken from the literature [59], the distribution of the volume fraction θ for our material model was determined as follows: The volume fraction for the RVE with the above characteristics is naturally defined as

$$\theta = \pi \sum_{i=1}^{16} r_i^2 \tag{25}$$

Since $\{r_i\}_{i=1}^{16}$ is a sample of independent normal random variables, it can be shown [60] that the sum in Eq. (25) is distributed as π times a noncentral chi-squared distribution with 16 degrees of freedom. The noncentrality parameter λ is given by

$$\lambda = \sum_{i=1}^{16} \left(\frac{\mu_i}{\sigma_i}\right)^2 \tag{26}$$

5.4. Numerical study

A preliminary study was carried out by running a series of ten experiments, each with $S = 100$ Monte Carlo simulations of the FRF. The frequency domain Ω ranges from 1 to 200 Hz. The resolution is 1 Hz, therefore $|\Omega| = N = 200$. The frequency 71 Hz was identified as consistently exhibiting the widest spread between its maximum and its minimum frequency response. This was the case for every one of the 10 repetitions of the experiment. Consequently, for 71 Hz fixed, the mean and variance of the FRF was computed for sample sizes S ranging from 1 to 2000. Fig. 4 shows that both the mean and the variance seem to stabilise around a sample size of 1000. Therefore, this value was chosen for S. The corresponding 1000 realisations are shown in Fig. 5.

The Monte Carlo mean and variance of the FRF at every $\omega \in \Omega$ were taken as the benchmark against which the accuracy of the emulation approach was compared. Note that it was the output

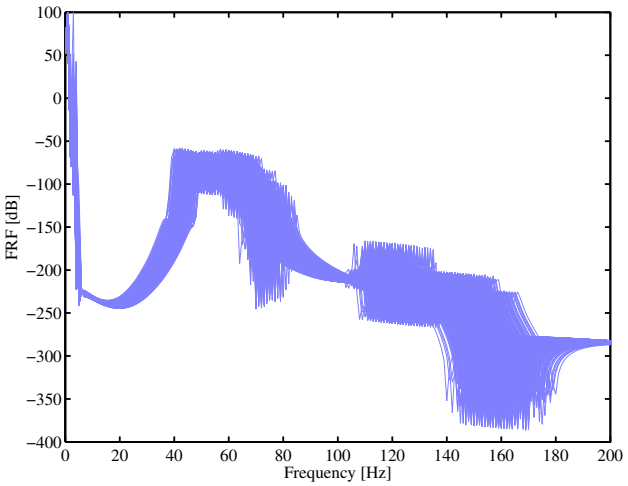

Fig. 5. The envelope resulting from $S = 1000$ Monte Carlo simulations of the frequency response simulator $\eta(\omega, \theta)$.

of the simulator, not the value of the quantity the simulator is attempting to predict, that was taken into account to determine the accuracy of the emulator approximation. The sizes of the sets of design points for each of the 1000 emulators corresponding to every frequency level had to be determined. Ideally, one should aim at having as many design points as possible to minimise the uncertainty in the output of the simulator. Intuitively, the more design points available, the maximum distance between any two design points either remains the same or decreases. If the amount of information increases, then the approximation would be bound to improve. It is therefore a choice of the modeller to decide between a better approximation and the use of computational resources. Since for each $\{\omega_\ell\}_{\ell=1}^{200}$ the functional form of $\eta(\omega, \theta)$ is unknown, an exploration of $\boldsymbol{\Theta}$ to determine every individual number of design points can be very costly. Instead, it was decided to take 100 design points for each emulator. This choice was made to show that the mean and the variance of the response can be estimated by generating only 10% of the original 1000 realisations of the FRF. Each set of design points was generated from the distribution of θ, a noncentral chi squared with 16 degrees of freedom and

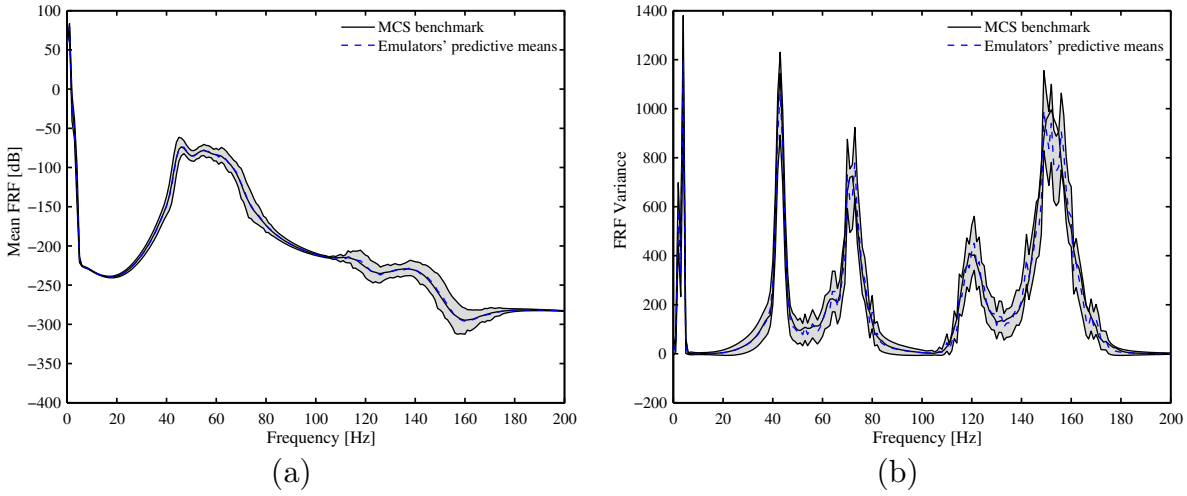

Fig. 6. Emulation and simulation of the mean frequency response (a) and variance of the frequency response (b). The emulation was performed for every frequency level in the input domain. The shaded areas represent 95% probability bounds.

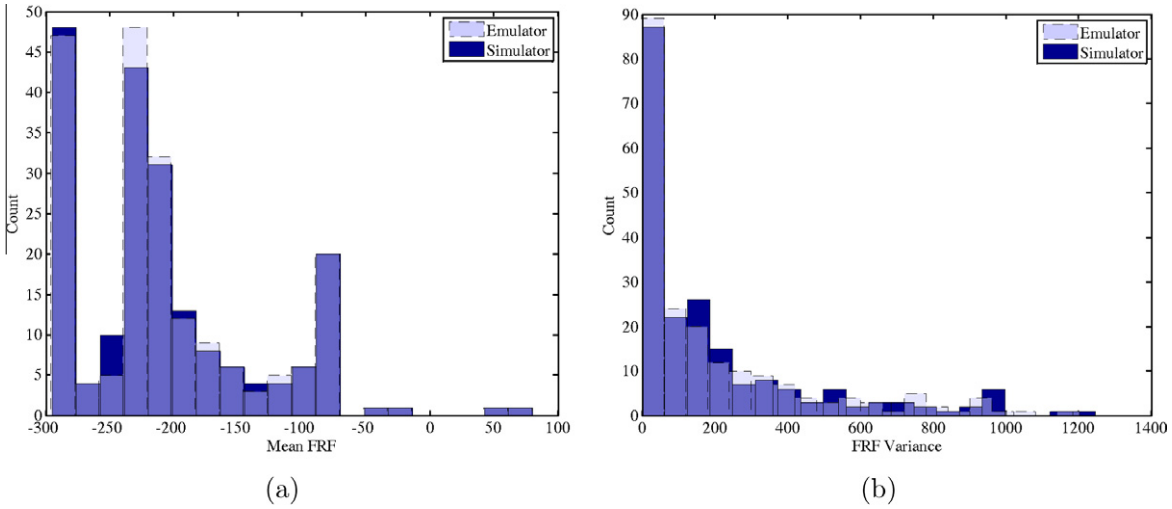

Fig. 7. Histograms of the simulated output mean (a) and variance (b) and of the emulated output mean (a) and variance (b). The degree of similarity of the distributions reflects the accuracy of the emulation strategy.

noncentrality parameter $\lambda = 64.43$. Due to the absence of prior knowledge, $\mathbf{h}(\omega,\theta) = 1$ was assumed for every emulator. The smoothness parameters were obtained by the maximum likelihood method outlined in [46,61].

Fig. 6(a) and (b) show, respectively, a comparison between the emulated mean and variance of the FRF against the MCS benchmark. The emulated curves were built with the nonparametric regression discussed in Section 4.2. They provide estimates of the mean and the variance for every frequency in 0–200 Hz. 95% probability bounds are also provided. There was an improvement in the computation time, due to the fact that the simulator was evaluated only $200 \times 100 = 20{,}000$ times, as opposed to $200 \times 1000 = 200{,}000$ times. Each emulator was run at virtually no computational cost. The saving in CPU time therefore implied a speed-up factor of around 10 when adopting the proposed approach.

Fig. 7 shows a comparison between the distributions of the simulated and emulated mean and variance for both strategies. Note how the histogram for the emulation strategy resembles that of MCS very closely for both statistics.

6. Conclusions

In this paper, Gaussian process emulators were employed as an effective approach to alleviate the cost of characterising the random response of a structure subject to vibration. This cost does not only arises from the need to obtain a large sample of responses for every frequency level in the selected domain, but also depends and is increased by the modelling of the material properties or by the presence of nonproportional damping. Hence, the selected case study was a nonproportionally damped plate made of a carbon fibre/epoxy composite material. We were able to model the uncertainty induced by the random diameter of each reinforcing carbon fiber as a non-central chi-squared distribution. We then propagated this uncertainty through a multiscale finite element model coupled with a Gaussian process emulator for each frequency level in order to estimate the mean and the variance of the frequency response of the plate.

It was shown that if the output of the simulator is treated as a function of the random parameter only, then it is possible to build an emulator at every point in the frequency domain and approximate the statistic of interest. The mean and the variance of the frequency response function estimated with Gaussian process emulators was benchmarked against a full Monte Carlo run. The metamodelling approach closely approximated the desired statistics, and the number of runs of the original expensive finite element simulator was reduced by one order of magnitude.

Acknowledgments

F.A. DiazDelaO, E.I. Saavedra Flores, and M.I. Friswell acknowledge funding from the European Research Council through Grant No. 247045 entitled "Optimisation of Multiscale Structures with Applications to Morphing Aircraft". E.I. Saavedra Flores also acknowledges the support of the Department of Civil Engineering, University of Santiago, Chile. S. Adhikari gratefully acknowledges the support of the Royal Society through the award of Wolfson Research Merit award.

Appendix A. Homogenisation-based multiscale constitutive theory

The main assumption in the homogenisation-based multiscale constitutive theories of solids is that the macroscopic or homogenised strain tensor $\boldsymbol{\varepsilon}$ at any arbitrary point $\mathbf{x}$ of the macroscopic continuum is the volume average of the microscopic strain tensor field $\boldsymbol{\varepsilon}_\mu$ over the domain Ω_μ of a representative volume element (RVE) of material. Similarly, the macroscopic or homogenised stress tensor field $\boldsymbol{\sigma}$ is assumed to be the volume average of the microscopic stress tensor $\boldsymbol{\sigma}_\mu$, over Ω_μ. Models of the present type can be found, for instance, in [62,54,63].

For any instant t, the above conditions can be expressed mathematically as

$$\boldsymbol{\varepsilon}(\mathbf{x},t) = \frac{1}{V_\mu}\int_{\Omega_\mu} \boldsymbol{\varepsilon}_\mu(\mathbf{y},t)\ \mathrm{d}V \quad \text{and} \quad \boldsymbol{\sigma}(\mathbf{x},t) = \frac{1}{V_\mu}\int_{\Omega_\mu} \boldsymbol{\sigma}_\mu(\mathbf{y},t)\ \mathrm{d}V \tag{A1}$$

in which V_μ is the volume of the RVE associated to point $\mathbf{x}$, and $\mathbf{y}$ is the local RVE coordinates. Furthermore, the microscopic strain tensor $\boldsymbol{\varepsilon}_\mu$ can be related to the local displacement field $\mathbf{u}_\mu$ by means of the standard expression $\boldsymbol{\varepsilon}_\mu \equiv \nabla^s \mathbf{u}_\mu$, in which ∇^s is the symmetric gradient operator. In addition, it is possible to decompose the displacement field $\mathbf{u}_\mu$ as a sum of a linear displacement $\boldsymbol{\varepsilon}(\mathbf{x},t)\mathbf{y}$, which represents a homogeneous strain, and a displacement fluctuation field $\tilde{\mathbf{u}}_\mu$. The displacement fluctuations field represents local variations about the linear displacement $\boldsymbol{\varepsilon}(\mathbf{x},t)\mathbf{y}$ and does not contribute to the macroscopic scale strain.

By taking into account the Hill–Mandel Principle of Macrohomogeneity [64,65], which establishes that the macroscopic stress power must equal the volume average of the microscopic stress power over Ω_μ, the virtual work equation for the RVE can be reduced to

$$\int_{\Omega_\mu} \boldsymbol{\sigma}_\mu(\mathbf{y},t) : \nabla^s \boldsymbol{\eta}\, \mathrm{d}V = 0 \tag{A2}$$

with $\boldsymbol{\eta}$ representing the virtual kinematically admissible displacements field of the RVE.

In order to make problem (A2) well-posed, a set of kinematical constraints upon the selected RVE is required. In what follows, the choice of this set will coincide with the widely used periodic boundary displacement fluctuations model, which is typically associated with the modelling of periodic media. Here, the fundamental kinematical assumption consists of prescribing identical displacement fluctuation vectors for each pair of opposite points $\mathbf{y}_+$ and $\mathbf{y}_-$ on the RVE boundary $\partial\Omega_\mu$, such that:

$$\tilde{\mathbf{u}}_\mu(\mathbf{y}_+,t) = \tilde{\mathbf{u}}_\mu(\mathbf{y}_-,t) \tag{A3}$$

By describing the RVE response by means of a generic local dissipative constitutive theory, the microscopic stress tensor $\boldsymbol{\sigma}_\mu$ is represented by a functional of the history of $\boldsymbol{\varepsilon}_\mu$, which is expressed symbolically as $\boldsymbol{\sigma}_\mu(\mathbf{y},t) = \mathfrak{F}_{\mathbf{y}}(\boldsymbol{\varepsilon}_\mu^t(\mathbf{y}))$. The functional $\mathfrak{F}_{\mathbf{y}}$ associated with point $\mathbf{y}$ maps the strain history, $\boldsymbol{\varepsilon}_\mu^t$, up to time t, into the stress $\boldsymbol{\sigma}_\mu$ of time t. In view of the above constitutive assumption and the additive decomposition of the microscopic displacement field, the equilibrium equation (A2) leads to

$$G(\boldsymbol{\varepsilon},\tilde{\mathbf{u}}_\mu,\boldsymbol{\eta}) \equiv \int_{\Omega_\mu} \mathfrak{F}_{\mathbf{y}}\{[\boldsymbol{\varepsilon}(\mathbf{x},t) + \nabla^s \tilde{\mathbf{u}}_\mu(\mathbf{y},t)]^t\} : \nabla^s \boldsymbol{\eta}\ \mathrm{d}V = 0 \tag{A4}$$

where we have defined G as virtual work functional.

References

[1] Bathe K-J. Finite element procedures. Englewood Cliffs, NJ, USA: Prentice Hall Inc.; 1995.
[2] Petyt M. Introduction to finite element vibration analysis. Cambridge, UK: Cambridge University Press; 1998.
[3] Ghanem R, Spanos P. Stochastic finite elements: a spectral approach. New York, USA: Springer-Verlag; 1991.
[4] Matthies HG, Brenner CE, Bucher CG, Soares CG. Uncertainties in probabilistic numerical analysis of structures and solids – stochastic finite elements. Struct Saf 1997;19(3):283–336.

[5] Shinozuka M, Yamazaki F. Stochastic finite element analysis: an introduction. In: Ariaratnam ST, Schuëller GI, Elishakoff I, editors. Stochastic structural dynamics: progress in theory and applications. London: Elsevier Applied Science; 1998.
[6] Adhikari S, Manohar CS. Transient dynamics of stochastically parametered beams. ASCE J Eng Mech 2000;126(11):1131–40.
[7] Haldar A, Mahadevan S. Reliability assessment using stochastic finite element analysis. New York, USA: John Wiley and Sons; 2000.
[8] Sudret B, Der-Kiureghian A. Stochastic finite element methods and reliability. Tech. rep. UCB/SEMM-2000/08, Department of Civil & Environmental Engineering, University Of California, Berkeley; November 2000.
[9] Nair PB, Keane AJ. Stochastic reduced basis methods. AIAA J 2002;40(8):1653–64.
[10] Scheidt JV, Purkert W. Random eigenvalue problems. New York: North Holland; 1983.
[11] Adhikari S, Friswell MI. Random matrix eigenvalue problems in structural dynamics. Int J Numer Methods Eng 2007;69(3):562–91.
[12] O'Hagan A. Bayesian analysis of computer code outputs: a tutorial. Reliab Eng Syst Saf 2006;91(10–11):1290–300.
[13] Keane A, Nair P. Computational approaches for aerospace design. Chichester, UK: John Wiley & Sons; 2005.
[14] Chowdhury R, Rao B. Assessment of high dimensional model representation techniques for reliability analysis. Probab Eng Mech 2009;24(1):100–15.
[15] Chowdhury R, Adhikari S. High-dimensional model representation for stochastic finite element analysis. Appl Math Model 2010;34(12):3917–32.
[16] Rao B, Chowdhury R. Enhanced high dimensional model representation for reliability analysis. Int J Numer Methods Eng 2009;77(5):719750.
[17] Rocha H. On the selection of the most adequate radial basis function. Appl Math Model 2009;33(3):1573–83.
[18] Haddad Khodaparast H, Mottershead JE, Badcock KJ. Propagation of structural uncertainty to linear aeroelastic stability. Comput Struct 2010;88(3–4):223–36.
[19] Khodaparast HH, Mottershead JE, Badcock KJ. Interval model updating with irreducible uncertainty using the Kriging predictor. Mech Syst Signal Process 2011;25(4):1204–26.
[20] Kleijnen JPC. Kriging metamodeling in simulation: a review. Eur J Oper Res 2009;192(3):707–16.
[21] Sacks J, Welch W, Mitchell T, Wynn H. Design and analysis of computer experiments. Statist Sci 1989;4(4):409–35.
[22] Santner T, Williams B, Notz W. The design and analysis of computer experiments. Springer series in statistics, London, UK; 2003.
[23] Challenor P, Hankin R, Marsh R. Avoiding dangerous climate change. Cambridge, UK: Cambridge University Press; 2006 [Ch. Achieving robust design from computer simulations, pp. 55–63].
[24] Rougier J. Probabilistic inference for future climate using an ensemble of climate model evaluations. Clim Change 2007;81(3):247–64.
[25] Kennedy MC, Anderson CW, Conti S, O'Hagan A. Case studies in Gaussian process modelling of computer codes. Reliab Eng Syst Saf 2006;91(10–11):1301–9.
[26] Haylock R, O'Hagan A. Bayesian statistics 5. Oxford, UK: Oxford University Press; 1996 [Ch. On inference for outputs of computationally expensive algorithms with uncertainty on the inputs].
[27] Oakley JE, O'Hagan A. Probabilistic sensitivity analysis of complex models: a Bayesian approach. J R Statist Soc B 2004;66(3):751–69.
[28] Kolachalama V, Bressloff N, Nair P. Mining data from hemodynamic simulations via Bayesian emulation. Biomed Eng Online 2007;6(47).
[29] DiazDelaO FA, Adhikari S. Structural dynamic analysis using Gaussian process emulators. Eng Comput 2010;27(5):580–605.
[30] Fricker TE, Oakley JE, Sims ND, Worden K. Probabilistic uncertainty analysis of an FRF of a structure using a Gaussian process emulator. Mech Syst Signal Process 2011;25(8):2962–75.
[31] Busby D. Hierarchical adaptive experimental design for Gaussian process emulators. Reliab Eng Syst Saf 2009;94(7):1183–93 [Special Issue on Sensitivity Analysis].
[32] Marrel A, Iooss B, Laurent B, Roustant O. Calculations of Sobol indices for the Gaussian process metamodel. Reliab Eng Syst Saf 2009;94(3):742–51.
[33] Bates R, Kennet R, Steinberg D, Wynn H. Achieving robust design from computer simulations. Qual Technol Quant Manage 2006;3(2):161–77.
[34] McFarland J, Mahadevan S. Multivariate significance testing and model calibration under uncertainty. Comput Methods Appl Mech Eng 2008;197(29–32):2467–79.
[35] Saavedra Flores EI, DiazDelaO FA, Friswell MI, Sienz J. A computational multi-scale approach for the stochastic mechanical response of foam-filled honeycomb cores. Compos Struct 2012;94(5):1861–70.
[36] DiazDelaO FA, Adhikari S. Gaussian process emulators for the stochastic finite element method. Int J Numer Methods Eng 2011;87(6):521–40.
[37] DiazDelaO FA, Adhikari S. Bayesian assimilation of multi-fidelity finite element models. Comput Struct 2012;92–93:206–15.
[38] Jacquelin E, Lainé J-P, Bennani A, Massenzio M. The anti-oscillator model parameters linked to the apparent mass frequency response function. J Sound Vib 2008;312(45):630–43.
[39] Caughey TK, O'Kelly MEJ. Classical normal modes in damped linear dynamic systems. Trans ASME J Appl Mech 1965;32:583–8.
[40] Meirovitch L. Principles and techniques of vibrations. New Jersey: Prentice-Hall International, Inc.; 1997.
[41] Géradin M, Rixen D. Mechanical vibrations. 2nd ed. New York, NY: John Wiely & Sons; 1997 [translation of: Théorie des vibrations].
[42] Adhikari S, Pastur L, Lytova A, Du-Bois JL. Eigenvalue-density of linear stochastic dynamical systems: a random matrix approach. J Sound Vib 2012;331(5):1042–58.
[43] Adhikari S, Chowdhury R, Friswell MI. High dimensional model representation method for fuzzy structural dynamics. J Sound Vib 2011;330(7):1516–29.
[44] Oakley J. Eliciting Gaussian process priors for complex computer codes. Statist 2002;51(1):81–97.
[45] Oakley J. Estimating percentiles of computer code outputs. Appl Statist 2004;53:83–93.
[46] Hankin RKS. Introducing BACCO, an R bundle for Bayesian analysis of computer code output. J Statist Softw 2005;14(16):1–21.
[47] Kennedy MC, O'Hagan A. Bayesian calibration of computer models. J R Statist Soc Ser B Statist Methodol 2001;63(3):425–50.
[48] Krzanowski W. Principles of multivariate analysis. Oxford, UK: Oxford University Press; 2000.
[49] Oakley JE, O'Hagan A. Bayesian inference for the uncertainty distribution of computer model outputs. Biometrika 2002;89:769–84.
[50] Rasmussen CE, Williams KI. Gaussian Processes for Machine Learning. The MIT Press; 2006 [Massachusetts Institute of Technology, 1971].
[51] Newland DE. Mechanical vibration analysis and computation. New York: Longman, Harlow and John Wiley; 1989.
[52] Adhikari S. Modal analysis of linear asymmetric non-conservative systems. ASCE J Eng Mech 1999;125(12):1372–9.
[53] Adhikari S. Optimal complex modes and an index of damping non-proportionality. Mech Syst Signal Process 2004;18(1):1–27.
[54] de Souza Neto EA, Feijóo R. Variational foundations of large strain multi-scale solid constitutive models: kinematical formulation. In: Advanced multi-scale material modelling: from classical to multi-scale techniques. Chichester: Wiley; 2010.
[55] Giusti SM, Blanco PJ, de Souza Neto EA, Feijóo RA. An assessment of the Gurson yield criterion by a computational multi-scale approach. Eng Comput 2009;26(3):281–301.
[56] Pellegrino C, Galvanetto U, Schrefler BA. Numerical homogenization of periodic composite materials with non-linear material components. Int J Numer Methods Eng 1999;46:1609–37.
[57] Speirs DCD, de Souza Neto EA, Perić D. An approach to the mechanical constitutive modelling of arterial tissue based on homogenization and optimization. J Biomech 2008;41:2673–80.
[58] Herakovich CT. Mechanics of fibrous composites. John Wiley & Sons; 1997.
[59] Everett R, Chu J. Modeling of non-uniform composite microstructures. J Compos Mater 1993;27:1128–44.
[60] Johnson NS, Kotz S, Balakrishnan N. Continuous univariate distributions, vols. 1–2. New York: John Wiley and Sons; 1995.
[61] Haylock R. Bayesian inference about outputs of computationally expensive algorithms with uncertainty on the inputs. PhD thesis, University of Nottingham, Nottingham, UK; 1996.
[62] Michel JC, Moulinec H, Suquet P. Effective properties of composite materials with periodic microstructure: a computational approach. Comput Methods Appl Mech Eng 1999;172:109–43.
[63] Saavedra Flores EI, de Souza Neto EA. Remarks on symmetry conditions in computational homogenisation problems. Eng Comput 2010;27(4):551–75.
[64] Hill R. A self-consistent mechanics of composite materials. J Mech Phys Solids 1965;13(4):213–22.
[65] Mandel J. Plasticité classique et viscoplasticité (Classic plasticity and viscoplasticity). CISM lecture notes, Udine, Italy: Springer-Verlag; 1971.